Electronic properties of half metallic Fe_3O_4 films

S. Jain and A. O. Adeyeye[a)]
Department of Electrical and Computer Engineering, Information Storage Materials Laboratory, National University of Singapore, Singapore 117576, Singapore

C. B. Boothroyd
Institute of Materials Research and Engineering, 3 Research Link, Singapore

(Received 1 November 2004; accepted 17 February 2005; published online 22 April 2005)

A systematic study of the electronic properties of Fe_3O_4 films grown directly on Si(001) substrates and on Ta, Ti, and SiO_2 buffer layers using electron beam deposition is presented. The effect of the buffer layer on the Verwey transition temperature and on the current–voltage characteristics of Fe_3O_4 has been studied in detail. We observed that for a fixed Fe_3O_4 film thickness, the Verwey transition temperature is strongly dependent on the buffer layer materials. Transmission electron microscopy reveals that the growth mechanism of the Fe_3O_4 films is strongly dependent on the type of buffer layer used. The contribution of long range and short range charge ordering below the transition temperature has also been investigated. We observed an insulator-like gap structure in the density of states below the transition temperature which gradually disappears with increasing temperature. © *2005 American Institute of Physics*. [DOI: 10.1063/1.1889247]

INTRODUCTION

Half metallic ferromagnetic materials, characterized by 100% spin polarization and having only one spin-subband at the Fermi level, have been the subject of interest for more than a decade.[1–4] Among all the half metallic ferromagnets, magnetite (Fe_3O_4) has gained enormous attention due to its high Curie temperature (T_c) of 858 K. Band structure calculations indicate that this spinel ferrite has only minority spin electrons at the Fermi level, indicating the half-metallicity of magnetite.[5,6] This means that for one spin orientation, Fe_3O_4 acts as a metal, while for the opposite orientation, it acts as an insulator. This property, in addition to the T_c, makes magnetite very attractive for room temperature applications in various spin-electronic devices, such as magnetic tunnel junctions for magnetic random access memory applications. The order-disorder transition at the Verwey point for magnetite is known to take place at ~120 K.[7] This metal–insulator transition of Fe_3O_4 makes its magnetoelectronic properties very interesting to investigate.

Several attempts have been made to characterize the bulk properties of Fe_3O_4 at low temperatures. Wei *et al.*[8] have studied the half metallic properties of epitaxially grown Fe_3O_4 films on (001) oriented MgO substrate using scanning tunneling spectroscopy. They observed that the half-metallic density of states of epitaxial Fe_3O_4 films exhibited a split in the energy spectra below the transition temperature. In another study, Ziese and Blythe[9] investigated the resistivity dependence with temperature for single crystal Fe_3O_4 and Fe_3O_4 films deposited on MgO substrates using Pulsed laser deposition. They established the relationship of conductivity with the Arrhenius law as a function of temperature below the metal–insulator transition. Recently, Liu *et al.*[10] reported a grain boundary dominated electron tunneling mechanism for the change in resistivity as a function of temperature for polycrystalline Fe_3O_4 films prepared by reactive sputtering. They observed that the Verwey transition associated with Fe_3O_4 materials does not appear for all the thicknesses of Fe_3O_4 films deposited. This was attributed to the fact that the resistivity of the Fe_3O_4 films is grain boundary controlled.

In this article, we have investigated, in a systematic way, the correlation between the metal–insulator transition of Fe_3O_4 films and the buffer layer materials. The films were grown directly on Si(001) substrates and also on Ta, Ti, and SiO_2 buffer layers. We observed that the metal–insulator transition of Fe_3O_4 is significantly modified by the buffer layer materials. This may be due to the stress imposed by the buffer layer and by impurity conduction. Transmission electron microscopy shows that the Fe_3O_4 growth is markedly influenced by the type of buffer layer used. For Fe_3O_4 films deposited on an SiO_2 buffer layer, the growth is columnar in contrast to other buffer layers. We have also investigated the current–voltage (I–V) characteristics of Fe_3O_4 as a function of temperature for each of the buffer layers. We observed that the low temperature conductivity of Fe_3O_4 is mediated by the exchange of ferrous and ferric ions, and is strongly dependent on the buffer layer materials.

EXPERIMENTAL DETAILS

Fe_3O_4 films were deposited using electron beam deposition from Fe_3O_4 pellets. The base pressure was maintained at 4×10^{-7} Torr with substrate temperature at 50 °C. The Si(001) substrates were first precleaned in acetone followed by isopropanol before loading in the deposition chamber. We deposited 150 nm thick Fe_3O_4 films at a rate of 0.8 Å/s directly on Si(001) substrates and on 20 nm Ta, Ti, and SiO_2 buffer layers. The deposition rate for Ta was 0.15 Å/s, for Ti it was 0.1 Å/s and for SiO_2, the rate was 0.3 Å/s. Details of the sample description are listed in Table I. Phase identification and crystal structure of Fe_3O_4 films were examined by

[a)]Author to whom correspondence should be addressed; electronic mail: eleaao@nus.edu.sg

TABLE I. Description of the various samples used in the experiments.

Sample name	Film structures
A	$Si(001)/Fe_3O_4(150\ nm)$
B	$Si(001)/Ta(20\ nm)/Fe_3O_4(150\ nm)$
C	$Si(001)/Ti(20\ nm)/Fe_3O_4(150\ nm)$
D	$Si(001)/SiO_2(20\ nm)/Fe_3O_4(150\ nm)$

conventional $\theta-2\theta$ x-ray diffraction scans using Cu Kα radiation. We observed that for Fe_3O_4 films deposited directly on Si(001), no obvious Fe_3O_4 peaks were found. However, for films deposited on Ta, Ti, and SiO_2 buffer layers, highly crystalline Fe_3O_4 with a preferred $\langle 311 \rangle$ orientation was obtained. This is in agreement with our earlier work.[11]

RESULTS AND DISCUSSION

The evolution during the metal–insulator transition has been investigated by analyzing the variation in the film's resistance as a function of temperature. Shown in Fig. 1 is the temperature dependence of the resistance for 150 nm Fe_3O_4 films deposited directly on a Si(001) substrate and on 20 nm of Ta, Ti, and SiO_2 buffer layers. We observed that at high temperatures, the resistance of Fe_3O_4 films deposited directly on Si(001) and on the Ta buffer layer is low. As the temperature decreases, the resistance increases drastically, nearly becoming an insulator. From the $R-T$ curve, we have determined the transition (T_v) for the Fe_3O_4 film on the Ta buffer layer and on the Si(001) substrate to be 32.5 and 65 K, respectively. The transition temperature is measured from the slopes of the curves obtained in Fig. 1. These metal–insulator transition points are lower when compared with the transition temperature proposed by Verwey[7] ($\sim$120 K). This decrease in T_v may be due to the impurities present at the interface between the buffer layer and the Fe_3O_4 films, thus making conduction possible even at such low temperatures. Impurity concentrations of less than 4% are known to increase the resistivity and also lower the temperature of the Verwey transition.[12] For Fe_3O_4 deposited directly on the Si(001) substrate however, we observed the presence of weakly coupled phases of Fe like FeO and Fe_2O_3 at the interface between Si and Fe_3O_4 using transmission electron microscopy. This unfavorable growth of an ionic oxide on a covalent substrate explains the introduction of a buffer layer between the Si substrate and Fe_3O_4 films. Thus, the conduction of Fe_3O_4 at temperatures below the Verwey transition temperature could be due to conduction through FeO and Fe_2O_3. This has been shown in our previous work where the different phases of Fe were also identified using x-ray photoelectron spectroscopy.[11]

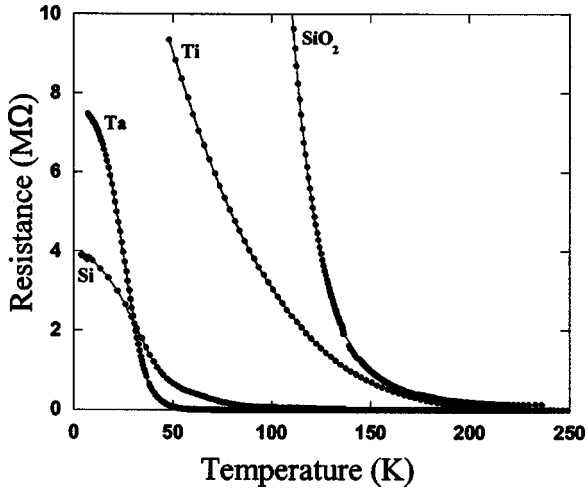

FIG. 1. Resistance vs temperature curves for 150 nm of Fe_3O_4 deposited on a Si(001) substrate and on Ta, Ti, and SiO_2 buffer layers.

TABLE II. Activation energies E_a calculated for Fe_3O_4 deposited on the buffer layers, below and above the transition temperature T_v.

		Activation energy (E_a) (meV)	
Sample name	T_v (K)	$T>T_v$	$T<T_v$
A	65.0	17	70
B	32.5	40	170
C	123.5	190	330
D	155.5	2	100

Figure 1 also shows the corresponding $R-T$ curves for Fe_3O_4 films deposited on Ti and SiO_2 buffer layers. For 150 nm of Fe_3O_4 film deposited on a Ti buffer layer, however, T_v is deduced to be 123.5 K, which is very close to the Verwey transition temperature. The increase in resistance from high temperatures to low temperatures does not show a sharp transition, but a gradual one. Surprisingly, for Fe_3O_4 films deposited on SiO_2 buffer layers, T_v increases to 155.5 K. The resistance shows a sharp jump at the transition temperature for the SiO_2 buffer layer. One possible explanation for the marked increase in T_v could be attributed to the stress induced by the buffer layer film. The transition temperatures for all the samples are listed in Table II.

The conductivity of magnetite film is known to be due to the exchange of electrons between the ferrous and ferric ions in the octahedral lattice sites, and thus the random distribution of the ions above the transition leads to an isotropic conductivity. Below the transition, however, the conductivity should be anisotropic. The energy required for the exchange of ferrous and ferric ions for conductivity to take place is called the activation energy. Table II lists the activation energies (E_a) for temperature ranges above and below T_v extracted from a fit of a thermally activated resistivity equation

$$\rho = \rho_0 \exp(E_a/kT), \tag{1}$$

where E_a is the activation energy, k is the Boltzman constant, T is the temperature and ρ_0 is the resistivity constant. For sample A the activation energy E_a, changes from 17 meV above T_v to 70 meV below T_v. The decrease of 53 meV in the energy gap around T_v is consistent with the 2 order of magnitude conductivity jump. Similarly, for sample B, E_a was deduced to be 40 and 170 meV, above and below T_v, respectively. The change of 130 meV in the E_a is large when compared to Fe_3O_4 films deposited on Ta buffer layers (53 meV), and is probably due to impurity conduction. For sample C, the conductivity activation energy E_a increases from 190 to 330 meV for temperatures above and below T_v.

Finally, for sample D, we observed an increase in E_a from 2 to 100 meV, above and below T_v, respectively.

In order to get a comprehensive understanding of the electrical properties of Fe_3O_4 at low temperatures, we have investigated the conductivity of Fe_3O_4 on different buffer layers by studying the $I-V$ characteristics using the four point probe method. By sourcing voltage and measuring the tunneling current, we have observed a sharp transition from an insulator gap to a peak structure around zero voltage.

It has been reported by Hibma *et al.*[13] that Fe_3O_4 has antiphase boundaries with Fe grains surrounded by oxide shells. At low temperatures, tunneling of electric charge into the grains increases the Coulomb energy by a charging effect. This opens the Coulomb gap and strongly enhances the tunnel resistance. The $I-V$ characteristics of such a configuration display a current step known as the Coulomb gap or an insulating gap that increases in width with decreasing temperature. This gap has been detected by photoemission,[14,15] optical,[12] and tunneling spectroscopy. Figure 2 shows the representative current–voltage plots for Fe_3O_4 deposited directly on an Si(001) substrate.

We observed a clear linear relationship between current and voltage at room temperature (well above T_v). As the temperature is decreased towards T_v, a region of low conductance starts to appear, in the form of a Coulomb gap or insulating gap, as shown in Fig. 2(b). Below T_v, the highest Coulomb gap we observed was 3.2 V at 15 K.

Figure 3 shows the representative $I-V$ curves for 150 nm of Fe_3O_4 deposited on 20 nm of Ta buffer layer. At temperatures above T_v, Fe_3O_4 is a relatively good spin polarized conductor showing a linear relation between voltage and current. However, as the temperature is decreased, the conductivity of Fe_3O_4 also decreases as seen by the increasing nonlinear behavior in current–voltage loops at 160 K. The inset in Fig. 3(a) shows the peak like structure above T_v. This peak structure gradually opens up in the form of an insulating gap as the temperature decreases. At the onset of T_v, the flat region around 0 V becomes more pronounced, thus showing a sharp decrease in conductivity. From Fig. 3(b) the Coulomb gap is found to be 1 V at 50 K. We observed a drastic change in the conductance of Fe_3O_4 in the temperature interval from 30 to 10 K, corresponding to an insulating gap of 5–10.5 V, respectively. A clear change in the conductivity spectrum can be seen in the inset. The inset in Fig. 3(c) is the region of low conductance which sets in below T_v. The abrupt change in the tunneling spectra from a linear conductivity behavior above T_v to the region of low conductance below T_v is a manifestation of the metal–insulator transition in the film. The threshold voltage for the coulomb gap is observed to be symmetric around 0 V.

Figure 4 shows the current–voltage characteristics for Fe_3O_4 films deposited on Ti buffer layers at various temperatures above and below T_v. The $I-V$ characteristics near room temperature show that the conduction spectra does not have a peak like structure, suggesting the conductivity to be dominated by antiphase boundaries with different interparticle junction parameters. Furthermore, the conductance of Fe_3O_4 shows a broadened peak structure at T_v, as seen in the inset of Fig. 4(b). We observed that the low conductivity region at

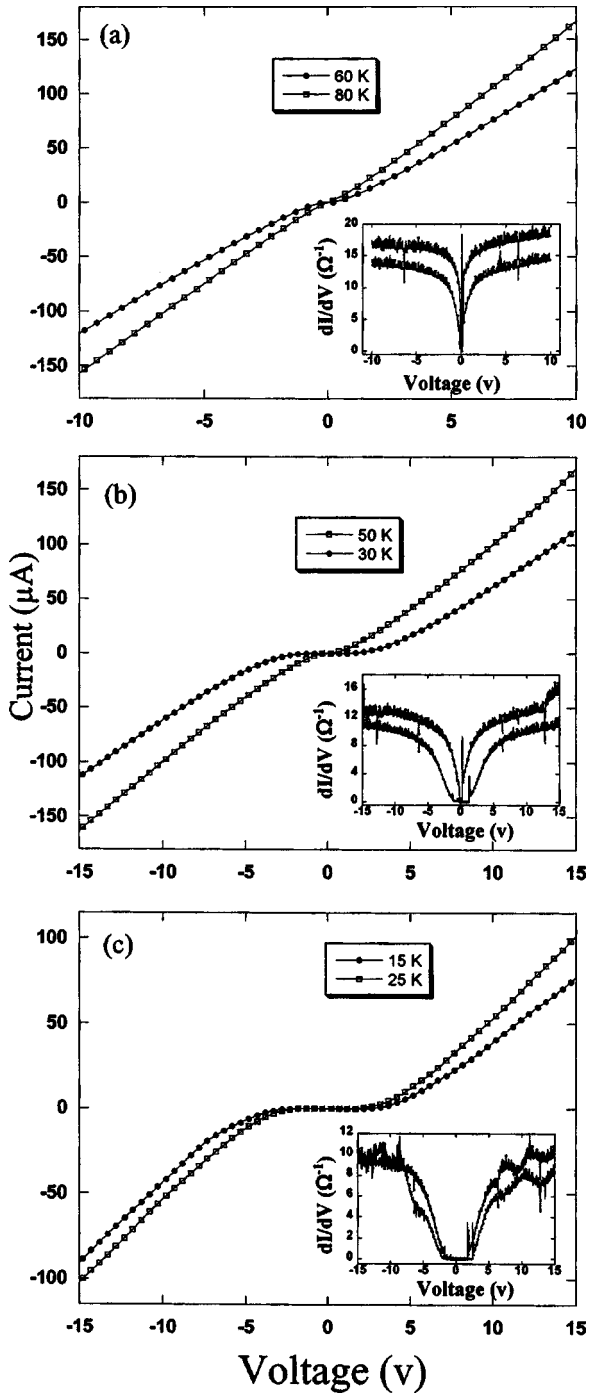

FIG. 2. $I-V$ characteristics for 150 nm films of Fe_3O_4 deposited on Si at: (a) 60, 80 K, (b) 30, 50 K, and (c) 15, and 25 K.

50 K, well below T_v, has an insulating gap of 19 V. This large insulating gap could be attributed to the microstructure of the Fe_3O_4 film deposited on the Ti buffer layer. Transmission electron microscope (TEM) analysis shows that the grain size of Fe_3O_4 on the Ti buffer layer is very small, explaining the above observation.

Figure 5 shows the representative $I-V$ curves as a function of temperature for Fe_3O_4 films deposited on SiO_2 buffer layers. As seen from the figure, the Coulomb gap is asymmetric starting from 0 V when compared with the symmetric behavior obtained for Fe_3O_4 films deposited on Ta and Ti buffer layers. The asymmetric nature of the Coulomb gap

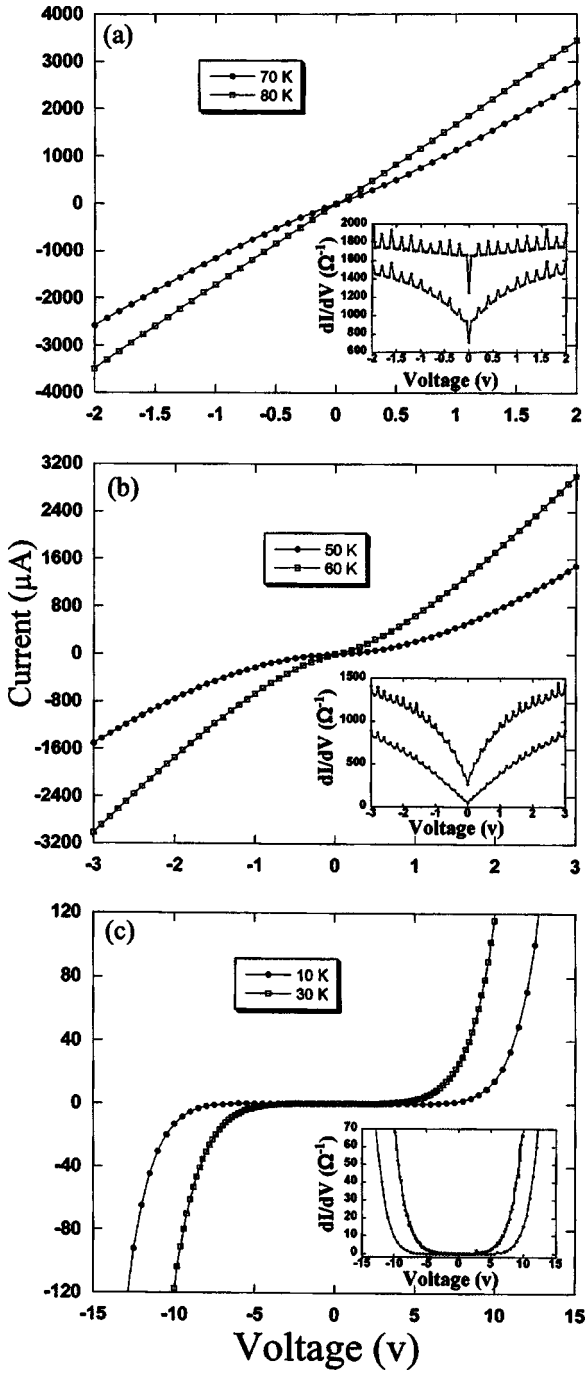

FIG. 3. $I-V$ characteristics for 150 nm films of Fe_3O_4 deposited on a Ta buffer layer at: (a) 70, 80 K, (b) 50, 60 K, and (c) 10, and 30 K.

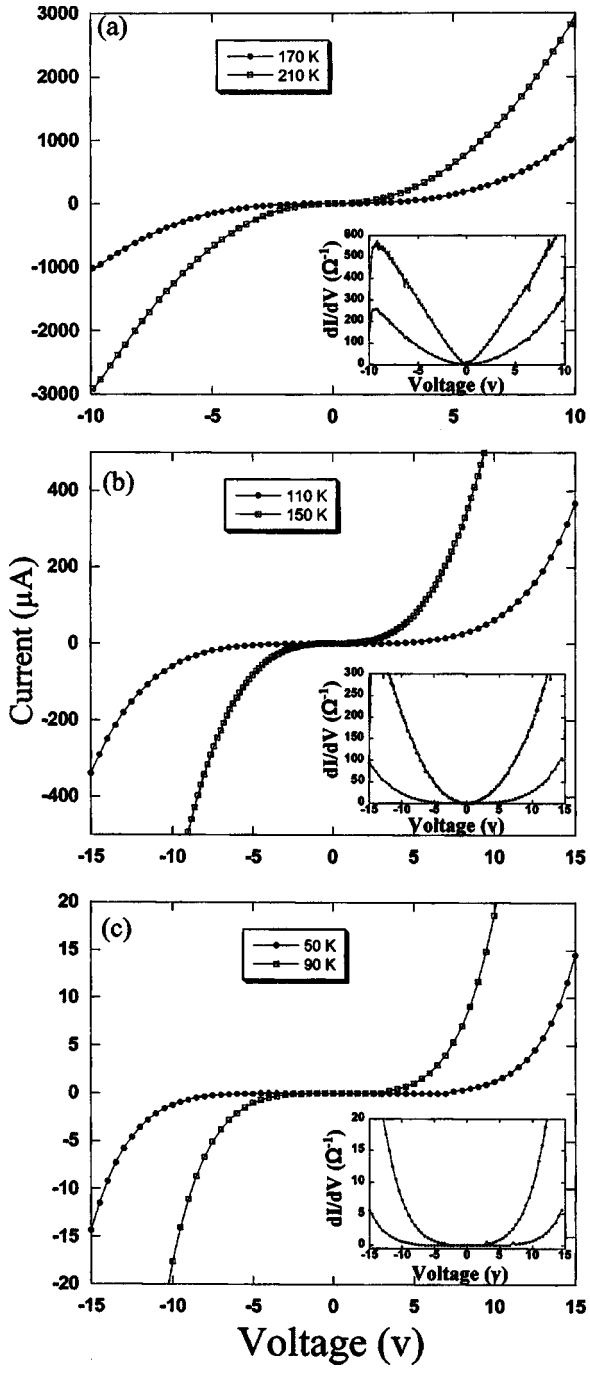

FIG. 4. $I-V$ characteristics for 150 nm films of Fe_3O_4 deposited on Ti at: (a) 170, 210 K, (b) 110, 150 K, and (c) 50, and 90 K.

may be due to the presence of impurities and voids in the grain structure. We observed that the Coulomb gap increases from 200 mV to 1 V when the temperature is decreased from 140 to 120 K. Below T_v we observed the highest Coulomb gap of 4.8 V at 105 K as shown in Fig. 5(c).

To investigate this asymmetric behavior of Fe_3O_4 when deposited on SiO_2 buffer layers, we characterized the interface properties and growth mechanism of Fe_3O_4 using TEM. Figure 6(a) shows a cross sectional bright field TEM micrograph of Fe_3O_4 deposited on a SiO_2 buffer layer. We clearly observed the columnar growth of Fe_3O_4 which is in direct contrast to the noncolumnar growth of Fe_3O_4 when deposited on Ta or Ti buffer layers (not shown). The exact conduction mechanism is still not known, but it is suggested that the columnar growth of Fe_3O_4 may be responsible for the asymmetric nature in the $I-V$ characteristic curves. Figure 6(b) is a high resolution TEM micrograph of the same sample.

CONCLUSIONS

We have presented the results of our investigation on the effect of buffer layer materials on the electronic conductivity of Fe_3O_4. We observed marked variations in the Verwey transition temperature for Fe_3O_4 films deposited on different buffer layers. The low temperature conductivity of Fe_3O_4 has

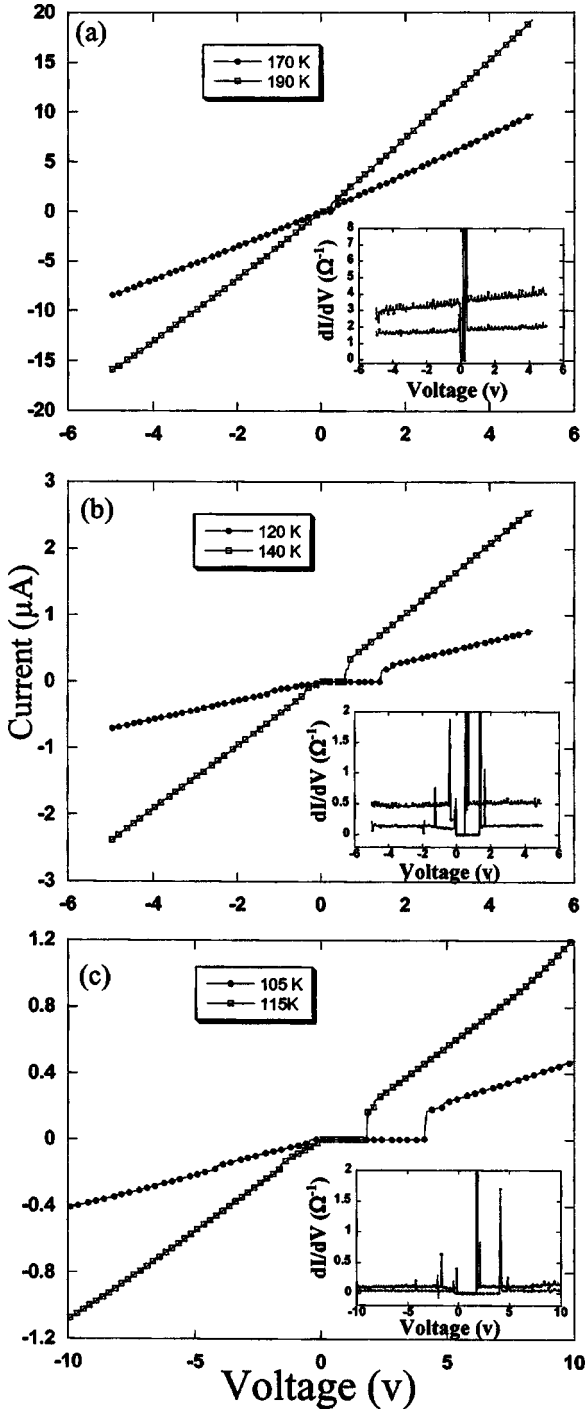

FIG. 5. $I-V$ characteristics for 150 nm films of Fe_3O_4 deposited on SiO_2 at: (a) 170, 190 K, (b) 120, 140 K, and (c) 105, and 115 K.

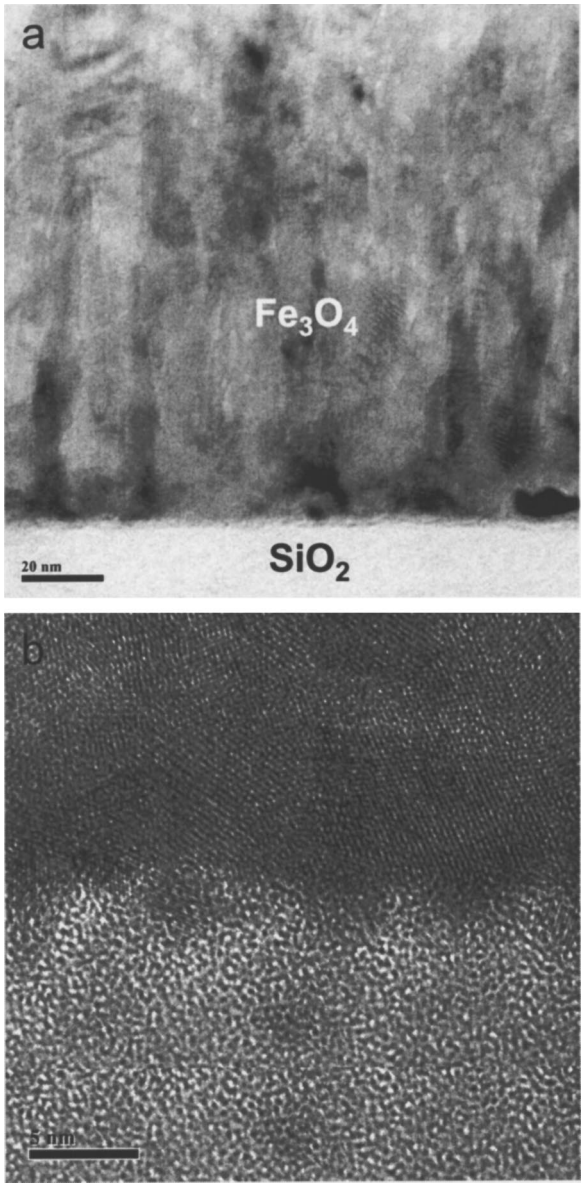

FIG. 6. (a) Cross sectional TEM micrograph showing 150 nm of Fe_3O_4 deposited on a 20 nm SiO_2 buffer layer. (b) High resolution image of the interface.

been investigated using $I-V$ characteristic measurements. A prominent Coulomb gap below the transition temperature was observed. For Fe_3O_4 films deposited on Si(001) substrates and on Ti and Ta buffer layers, the Coulomb gap is symmetric, compared with the asymmetric gap observed for films deposited on SiO_2 buffer layers. We have thus shown that the metal–insulator transition temperature can be significantly modified by changing the buffer layer material.

ACKNOWLEDGMENTS

This work was supported by National University of Singapore (NUS) Grant No. R263-000-283-112. One of the authors (J.S.) would like to thank NUS for her research scholarship.

[1]R. A. Groot and F. M. Muller, Phys. Rev. Lett. **50**, 2024 (1983).
[2]P. G. van Engen, K. H. Buschow, and R. Jongebrevr, Appl. Phys. Lett. **42**, 202 (1983).
[3]R. A. Groot and K. H. Buschow, J. Magn. Magn. Mater. **54–57**, 1377 (1986).
[4]V. Y. Irkhin and M. I. Katsnel'son, Phys. Usp. **37**, 659 (1994).
[5]Z. Zhang and S. Satpathy, Phys. Rev. B **44**, 13319 (1991).
[6]Y. Yanase and K. Siratori, J. Phys. Soc. Jpn. **53**, 312 (1984).
[7]E. J. W. Verwey, Nature (London) **144**, 327 (1939).
[8]J. Y. T. Wei, N. C. Yeh, R. P. Vasquez, and A. Gupta, J. Appl. Phys. **83**, 7366 (1998).
[9]M. Ziese and H. J. Blythe, J. Phys.: Condens. Matter **12**, 13 (2000).
[10]H. Liu, E. Y. Jiang, H. L. Bai, R. K. Zheng, and X. X. Zhang, J. Phys. D **36**, 2950 (2003).
[11]S. Jain, A. O. Adeyeye, and D. Y. Dai, J. Appl. Phys. **95**, 7237 (2004).
[12]J. H. Park, L. H. Tjeng, J. W. Allen, P. Metcalf, and C. T. Chen, Phys. Rev. B **55**, 12813 (1997).
[13]T. Hibma, F. C. Voogt, L. Niesen, P. A. A. van der Heijden, W. J. M. de

Jonge, J. J. T. M. Donkers, and P. J. van der Zaag, J. Appl. Phys. **85**, 5291 (1999).
[14]A. Chainani, T. Yokaya, T. Morimoto, T. Takahashi, and S. Todo, Phys. Rev. B **51**, 017976 (1995).
[15]L. V. Gasparov, D. B. Tanner, D. B. Romero, H. Berger, G. Margaritondo, and L. Forro, Phys. Rev. B **62**, 7939 (2000).